Bond order effects in electromechanical actuation of armchair single-walled carbon nanotubes

Tissaphern Mirfakhrai,[1,a)] Rahul Krishna-Prasad,[2] Alireza Nojeh,[2] and John D. W. Madden[1]
[1]*Department of Electrical and Computer Engineering and Advanced Materials and Process Engineering Laboratory, University of British Columbia, Vancouver, British Columbia V6T 1Z4, Canada*
[2]*Department of Electrical and Computer Engineering, University of British Columbia, Vancouver, British Columbia V6T 1Z4, Canada*

(Received 11 May 2009; accepted 16 December 2009; published online 17 February 2010)

In this paper we first use *ab initio* simulations to study the strains induced by charging an armchair (5,5) carbon nanotube (CNT) segment. The observed behavior is far from a monotonic expansion that one might have expected from a classical point of view. Subsequently a new method is proposed to predict the nonelectrostatic part of the electromechanical actuation response of the nanotube based on the spatial distribution of its molecular orbitals. Locally bonding and locally antibonding molecular orbitals are defined for the CNT segment structure based on analogy with bonding and antibonding orbitals in diatomic molecules. The nonmonotonic overall actuation is explained based on the above proposition and the general alignment of the expanding and contracting bonds with respect to the axis or circumference of the CNT segment. Using the well-known concept of bond order, the actuation of this complex system of many atoms is predicted with close quantitative agreement with the *ab initio* simulations. © *2010 American Institute of Physics*.
[doi:10.1063/1.3290200]

I. INTRODUCTION

Carbon nanotubes (CNTs) can be thought of as rolled-up sheets of graphene with nanometer-sized diameters and lengths that have reached several millimeters. Single-walled nanotubes (SWNTs) consist of one such rolled-up sheet. The electronic and mechanical properties of CNTs have been studied extensively since their discovery in 1991. Simulations and experiments have shown that CNTs are very stiff for their diameter, having Young's moduli in the terapascal range[1] and have tensile strengths of about 60 GPa,[2] far higher than in any bulk material.

In 1999 it was discovered that a sheet of entangled CNTs ("Bucky paper") submersed in an electrolyte expands and contracts (actuates) when the voltage applied to it is changed.[3] It had been experimentally known since the 1960s (Ref. 4) that the C–C bond length in ion-intercalated graphite varies when the degree of charging of the constituent graphene sheets is changed. It has therefore been speculated that the actuation in CNTs is also the result of C–C bond length changes, rather than intertube effects. More recently, some macroscopic CNT structures such as fibers[5] and yarns[6] of CNTs have been shown to contract[7] rather than expand, even at relatively high charge levels. This discovery makes it necessary to further investigate the mechanisms of actuation of individual CNTs, which are likely a combination of Coulombic repulsion and quantum chemical effects. Such studies, when coupled with the geometry of the macroscopic structures, will help us understand the actuation of CNTs and pave the way for applications.

We have previously used *ab initio* methods in GAUSSIAN 03 software[8] to study the electromechanical actuation resulting from charging a (5,5) SWNT segment, consisting of 120 atoms, terminated by H atoms.[9] The Hartree–Fock (HF) method was used as the method of simulation using a 6-31G(d) basis set. The results for axial and radial strains are plotted in Fig. 1. A charge level of +1 $|e|$ means that one electron has been removed from the system, while −1 $|e|$ implies one electron added. These correspond to +0.01 and −0.01 $|e|$/atom charge levels, respectively, in our previous paper.[9]

The piecewise-linear shape of the plot is to some extent counterintuitive, especially when compared with smooth curves expected from classical Coulomb effects, such as in Ref. 10. As we have previously suggested, this behavior clearly corresponds to the filling of molecular orbitals (MOs) in the CNT segment. As electrons are added or removed from the simulated CNT segment it is found that the change in strain per electron is nearly constant for the filling of a given MO (e.g., when charge is increased from 0 to 1 to 2 $|e|$). The slope then changes abruptly when the transition is made to the occupancy of a new MO. This effect is evident in Fig. 1, where abrupt changes in slope (or "jags") are observed each time the second electron is added (e.g., at $q = \pm 2$ $|e|$ or $q = \pm 4$ $|e|$). Therefore, we argue that the strain-charge plot will still consist of such three-point line segments even for longer nanotube structures. However, changes in slope may become less abrupt as energy levels are expected to be closer together for longer CNTs, and MOs would be more delocalized. As a result, the strain-charge curves may look smoother.

Our previous work showed the existence of this correlation between orbital filling and strain. In this work we seek to provide an explanation for this effect and to quantify its

a)Electronic mail: tissa@ece.ubc.ca.

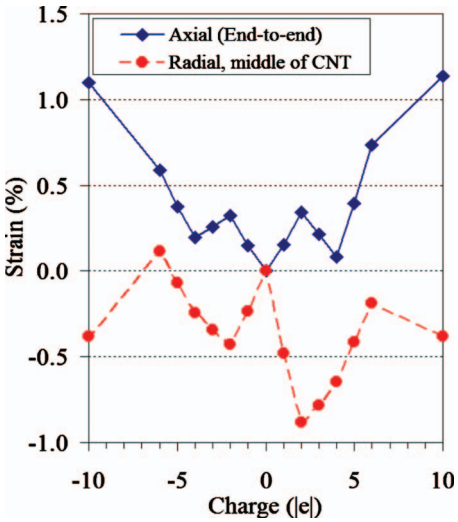

FIG. 1. Axial and radial strains induced by adding or removing electrons from the CNT segment. Both axial and radial strains consist of line segments of three points on an almost straight line, jointed to the neighboring line segments at an angle.

extent. Here, we present a more intuitive argument to relate the shape of the strain-charge relationship to the spatial distribution of the MOs over the CNT segment under study. We draw upon the basic concepts of bonding and antibonding orbitals and bond order (BO), typically used for small molecules, to describe the actuation behavior of the complex CNT segment structure. The simulations on which the analysis is based have been previously published.[9]

II. BACKGROUND: BOND ORDER AND ACTUATION

Bonding MOs in diatomic molecules are formed by adding two atomic orbitals, one from each atom, and therefore, there is a finite and nonzero probability of finding the electron in the space between the nuclei. Bonding MOs thus have spatial distributions aligned with the bond and with no node between the two nuclei (Figs. 1.5 and 1.8a in Ref. 11). On the other hand, *antibonding* MOs are formed by subtraction of atomic orbitals belonging to the two nuclei and their spatial distributions form lobes of opposite phases around the nuclei, separated by a nodal plane that crosses the bond (Figs. 1.6 and 1.8b in Ref. 11). Bonding orbitals generally help stabilize a molecule while the antibonding configurations are repulsive, and tend to split the molecule apart. Both bonding and antibonding configurations can be present in the ground state of a molecule providing that the configuration is energetically favorable.

The relationship between bond length and the occupancy of bonding and antibonding orbitals contributing to the bond has been studied before, sometimes using the concept of BO. *Formal* BO has been defined as half of the difference between the number of electrons in bonding and antibonding orbitals contributing to the bond. This definition is somewhat *ad hoc* and an exact, quantum-mechanical definition for BO has been debated extensively in the literature. (see Refs. 12 and 1–18 therein). BO in carbon compounds has been studied in the past. Pauling[13] showed that a change in BO results in a change in the bond length through the following empirical relationship:

$$\Delta L = -2 \times 0.353 \log(\mathrm{BO}), \tag{1}$$

where BO is the bond order, and ΔL is the difference between the length of a bond with order of BO and that of a single carbon-carbon (C–C) bond as in ethane for which BO=1. The factor of 2 on the right-hand side of Eq. (1) has been introduced because we have taken the change in the distance between the two carbon atoms (ΔL) instead of Pauling's original atomic radius (ΔR) as the parameter of interest. Coulson and Taylor[14] calculated the BO of the C–C bond in graphene to be 1.525. Kakitani[15] determined the BO in benzene ring to be 1(2/3). Pietronero and Strässler[16] studied bond length changes due to charging in graphite intercalation compounds. They named BO changes along with (a) modification of the tight-binding matrix elements due to the fact that the atomic potential is changed, and (b) the Coulomb repulsion between the charged atoms as the factors contributing to bond length change. However, they assumed a uniform change of the bond length among all bonds, which could well be the case if the graphene sheet under study is very large. Their model is therefore inadequate in explaining the alternating expansive and contractile behavior observed in the simulated CNT segment. Verissimo-Alves *et al.*[17] qualitatively use the concept of bonding and antibonding orbitals to explain the discrepancy between their simulation results for CNT actuation and similar results for graphene. However, they use those terms in their traditional meaning to refer to MOs with energy levels lower or higher than the Fermi level, respectively. They use that argument to explain the general trends in the change of the lattice size in some CNTs they have simulated. This approach assumes an infinitely long CNT with uniform actuation in all unit cells throughout. Therefore no predictions about local changes in bond lengths can be made.

III. ACTUATION PREDICTIONS BASED ON BOND ORDER

Figure 2 shows the spatial distribution of the highest occupied molecular orbital (HOMO) and the lowest unoccupied molecular orbital (LUMO) of an uncharged (5,5) CNT segment at spin multiplicity of 1 (all electrons paired). Those spatial distributions are superimposed on the CNT segment structure showing the bonds. Blue and red colors indicate the positive and negative phases of the wave function. It can be seen that some C–C bonds in the nanotube are aligned with the electron clouds, while other bonds interconnect electron clouds of opposite phase, resulting in a nodal plane crossing the bond in the middle. These spatial shapes resemble bonding and antibonding MOs in diatomic molecules, respectively. We therefore speculate that when charge is added to the system, the local effect of these electron clouds on bond length may be like bonding or antibonding orbitals in diatomic molecules. We hereby show that in general the bonds aligned with the MO electron clouds contract (expand) upon the addition (removal) of an electron, while bonds on which the MO has a node expand (contract). Due to the geometry of

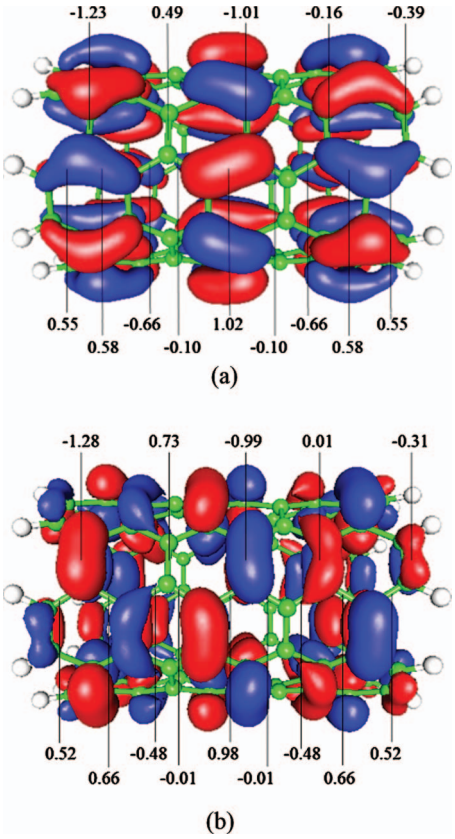

FIG. 2. Spatial distribution of (a) HOMO and (b) LUMO of an uncharged (5,5) CNT segment at spin multiplicity =1. The numbers indicate the change in length (%) of the corresponding bond upon taking an electron from HOMO (a) or adding an electron to LUMO (b)

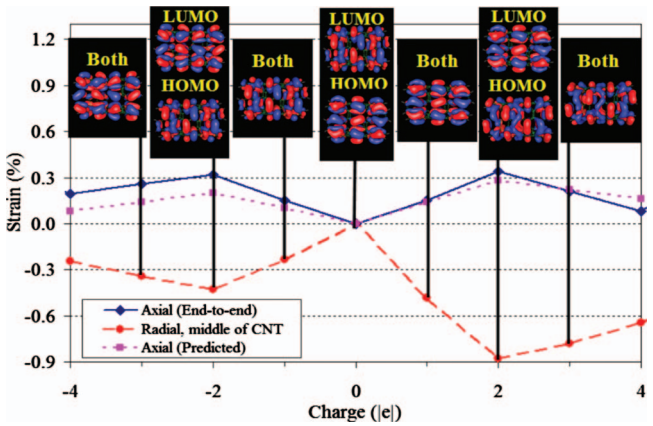

FIG. 3. Axial and radial strains in a (5,5) CNT segment induced as a result of charging

the CNT segment, and where those bonds are located along the length or circumference, the entire CNT segment will expand or contract axially or radially.

If an electron is taken from the uncharged CNT segment, that electron comes out of the HOMO level, which contains two electrons [Fig. 2(a)]. The electron clouds in this orbital are mostly aligned with the bonds along the CNT axis. Therefore, we predict that the removal of an electron from this orbital would lead to an expansion of those bonds, and an axial expansion of the CNT segment. Meanwhile, the same orbital has nodes on the bonds aligned with the circumference of the CNT segment, which interconnect electron clouds of opposite phase. Therefore the removal of an electron from this orbital is expected to make those bonds contract. The numbers written on bonds in Fig. 2(a) show the percent change in length of each bond, induced upon the removal of an electron from the MO. It can be seen that most of the bonds covered by the electron clouds are in fact expanding and most of the bonds aligned with the circumference contract when an electron is removed.

When an electron is added into the uncharged system (assuming full pairing of electrons of opposite spins in the uncharged state), it enters the LUMO, which is distributed mostly along the circumference of the CNT segment [Fig. 2(b)]. This time, the electron clouds are mostly aligned with the bonds along the circumference, while the nodes appear on bonds located along a zigzag path of carbon-carbon bonds running along the CNT axis. Let us assume that after the addition of an electron to the system, the energy levels and the spatial distributions of the orbitals with lower energies have not changed significantly. We therefore predict that the occupation of this MO is expected to result in an axial expansion. At the same time, since the electron clouds are aligned mostly circumferentially, a radial contraction is also expected. The numbers written on bonds in Fig. 2(b) show the percent change in length induced in each bond upon adding an electron to the MO. It can be seen that most of the bonds covered by the electron clouds in fact contract and most of the bonds along the length of the CNT expand when an electron is added. As expected, the phase of the wave function does not affect the direction or amplitude of the change in the bond length. It should be noted that bonds located at similar positions with respect to the CNT geometry and the electron clouds undergo similar strains. Therefore, the subset of bonds for which the strains are shown in Fig. 2 represents the strain behavior of all types of C–C bonds present in the CNT segment.

There are some circumferentially aligned bonds that seem to expand upon charge injection, even though there seems to be no node on them at first glance. The most striking example of these is the bond in the center-left of the structure, which has no electron cloud on it or its ends in Fig. 2, but is expanding by 0.49% and 0.73% when 1 electron is removed or added, respectively. Such behavior may be due to the heavily interconnected nature of the CNT. The lack of an electron cloud on the bond implies very low electron density around it. Meanwhile, all four bonds connected to the ends of the bond in question are contracting [two marked in Figs. 2(a) and 2(b) with strain values]. Since the bond itself has little electron density on it or its ends, the injection of an electron will have little direct effect on its length. However, it expands as it is pulled by the four bonds connected to its ends. The short length of the simulated CNT segment structure may also contribute to these anomalies in the actuation behavior.

Figure 3 shows a close up of the middle section of the plot in Fig. 1 with plots of the spatial distribution of the HOMO and LUMO orbitals superimposed on the CNT segment. It can be seen that, as predicted above, the CNT structure as a whole contracts radially (negative radial strain) and

expands axially (positive axial strain) upon gaining an extra electron (−1 |e|) or losing an electron (+1 |e|).

The HOMO has nodes on the bonds along the circumference of the CNT, and we have shown that those bonds contract when an electron is removed from the HOMO (It can be shown by looking at lower contour levels of the wave function that there are also nodes on the circumferentially aligned bonds in HOMO seemingly devoid of electron clouds, although, as discussed above, the effect of such nodes on strain is weak). Therefore, as far as bonds along the circumference are concerned, the HOMO behaves like an antibonding orbital. Meanwhile, bonds along the axis of the CNT expand when an electron is removed from HOMO and electron clouds in HOMO are aligned with the bonds along the CNT axis. Therefore, with respect to bonds along the CNT axis, the HOMO behaves like a bonding orbital. We therefore propose to call the HOMO *locally bonding* with respect to bonds along the length of the CNT segment, and at the same time, *locally antibonding* with respect to the bonds along the CNT circumference. Similarly, it can be said that the LUMO has a locally bonding nature with respect to the bonds aligned with the circumference of the CNT, while it has a locally antibonding nature with respect to the bonds oriented along the zigzag path along the CNT axis.

Let us now study the effect of adding two or more electrons to the system. When the first electron is added, the old LUMO (of the uncharged CNT) becomes the HOMO of the new system. This orbital still has room for another electron, and so a second electron added to the system will go into the same orbital. As shown above, adding an electron into this orbital is expected to result in axial expansion and radial contraction of the CNT segment. Adding a second electron in the same orbital will thus result in further axial expansion and radial contraction when we increase the charge from −1 to −2 |e|. At this point the HOMO is fully occupied, and so if a third extra electron is added to the system, it will have to go to a higher energy level orbital (labeled as LUMO in Fig. 3 at −2 |e|). This orbital is once again axially oriented compared with its predecessor; thus it is locally bonding with respect to bonds in the direction of the CNT segment axis and locally antibonding with respect to bonds along the circumference. As a result, the CNT segment is expected to contract axially and expand radially when the charge level is increased to −3 |e|. It can be seen that all of our predictions are confirmed by the *ab initio* results in Fig. 3. Similar arguments can be presented to predict the axial and radial strains for the cases where electrons are removed from the CNT segment to leave it with positive charge. These predictions are also confirmed by the *ab initio* results in Fig. 3.

Let us now try to quantify the strain predicted based on the change in the BO and occupancy, to see if it is compatible with the strains in individual bonds that we have found through simulation. Pauling's equation [Eq. (1)] can be rearranged to relate the change in bond length to the number of electrons contributing to the bond, relative to the bond length at $N_e=2$, i.e., $L_{\mathrm{BO}=1}$

$$L - L_{\mathrm{BO}=1} = -2 \times 0.353 \ln\left(\frac{N_e}{2}\right) \Big/ \ln(10) \cong -0.307 \ln\left(\frac{N_e}{2}\right)(\text{Å}), \tag{2}$$

where the value of $L_{\mathrm{BO}=1}$ has been experimentally measured to be around 1.542 Å. Then, if partial charge of ΔN_e is added to the bond, the resulting change in the bond length can be found through

$$\Delta L = -0.307 \ln\left(\frac{N_e + \Delta N_e}{N_e}\right) \cong -0.307 \frac{\Delta N_e}{N_e}. \tag{3}$$

Now let us direct our attention to Fig. 2(b), which shows the spatial distribution of the LUMO of our CNT segment. There are 40 pairs of electron clouds in the LUMO orbital, where each pair covers a single bond (one outside CNT segment and one inside). So let us simplistically assume that when 1 electron is added to the system, the extra electron is divided equally among the cloud pairs and therefore, each pair (and the bond corresponding to the pair) receives 1/40th of an electron. Any bond whose only one end is covered by the cloud is assumed to receive half of the electrons in the cloud, namely, 1/80th of an electron. Equation (3) can thus be used to predict actuation strains in each bond. Assuming the angles between the bonds do not change significantly during this charging process, the total axial actuation of the CNT segment can be computed by adding up the contribution to the CNT segment length from the change in the length of the bonds not fully aligned with the circumference. These are the bonds marked in Figs. 2(a) and 2(b), whose strain values are written below the figures. To consider the contribution from each bond, the angle it forms with the CNT segment axis must also be considered and the axial component of the bond strain must be taken into account. The result is the predicted curve in Fig. 3, almost perfectly replicating the behavior of the simulated CNT segment. The existing mismatch between the predicted strain and the simulation results can be attributed to a number of factors. Equation (1) is empirically suggested for uncharged diatomic molecules, and therefore, a separate Coulomb effect may be needed to explain actuation when the system under study has a net charge. Second, our model is based on the assumption that the electron added or removed only affects the MO with highest available energy level and that MOs with lower energies are not affected by the addition of charge. This assumption may not always be true and therefore, the energy levels and spatial distributions of the electron clouds of lower-energy MOs may also change as a result of adding charge to the higher-energy MOs, which could contribute to the actuation strain. Third, our assumption that the extra electron is equally divided among all electron clouds in an MO may not be acceptable at all charge levels, resulting in uneven length change among the bonds. At last, the strongly interconnected nature of the CNT segment structure also affects the strains, since unlike in diatomic molecules, where atoms have more freedom to move, bond lengths are here affected by the changes in adjacent bonds. The fact that our model closely predicts the electro-

mechanical strain-to-charge relationship in the CNT segment despite those effects shows that those effects are not significant at the charge levels under study and confirms the validity and success of our approach.

The present proposition seems to provide an intuitive explanation for the angular and jagged shapes of the strain responses presented in Fig. 1, which would otherwise be hard to explain or would have to be dismissed as simulation artifacts. Moreover, it shows how the basic concept of BO, more typically associated with chemistry of small molecules can be successfully applied to study the behavior of CNTs, most often studied with techniques adopted from solid-state physics. The success of our proposition in intuitively explaining the electromechanical response of an extended many-body system may point the direction for further research that may lead into a new way of looking at the responses of nanoelectromechanical systems, and provide us with more intuition for engineering structures that could generate larger actuation strains. This method may also be useful in studying the response of systems with large numbers of atoms other than CNTs, such as expansions induced in conducting polymers upon charging.

IV. FURTHER DISCUSSION

It is informative to verify the changes in the lengths of individual bonds during actuation. As an example, and due to the general symmetry within the CNT segment, only the results for a few bonds are studied here. Figure 4(a) shows the CNT segment structure with the locations of bonds studied highlighted with black lines. The changes in the lengths of those bonds were found both from our direct HF simulations and from BO calculations. The results are plotted in Figs. 4(b)–4(f). It was found that at all studied charge levels

$$L_{8-25} \cong L_{86-98},$$

$$L_{25-26} \cong L_{85-86},$$

$$L_{66-85} \cong L_{26-45},$$

$$L_{65-66} \cong L_{45-46},$$

where L_{m-n} represents the length of the bond between atoms numbered m and n, to an accuracy smaller than $10^{-6}\%$. This is not unexpected, since, as can be seen from Fig. 4(a), those bonds are located at similar distances from the CNT segment rim, and thus hold identical locations within the CNT segment. As can be seen from Figs. 4(b)–4(f), the qualitative behavior of all bond lengths as a function of charge is almost always predicted correctly. The quantitative mismatch between the bond length values found from HF and the BO approach may be due to reasons similar to those discussed in Sec. III for the mismatch in total CNT segment strains.

Another quantity of interest in studying actuation in CNTs is the radial strain. The radial strain from HF simulations is plotted in Fig. 1. As described in more detail in Ref. 9, the diameter used to define these strain values are defined using the distance between two carbon atoms opposite each other near the middle of the CNT segment. This definition is

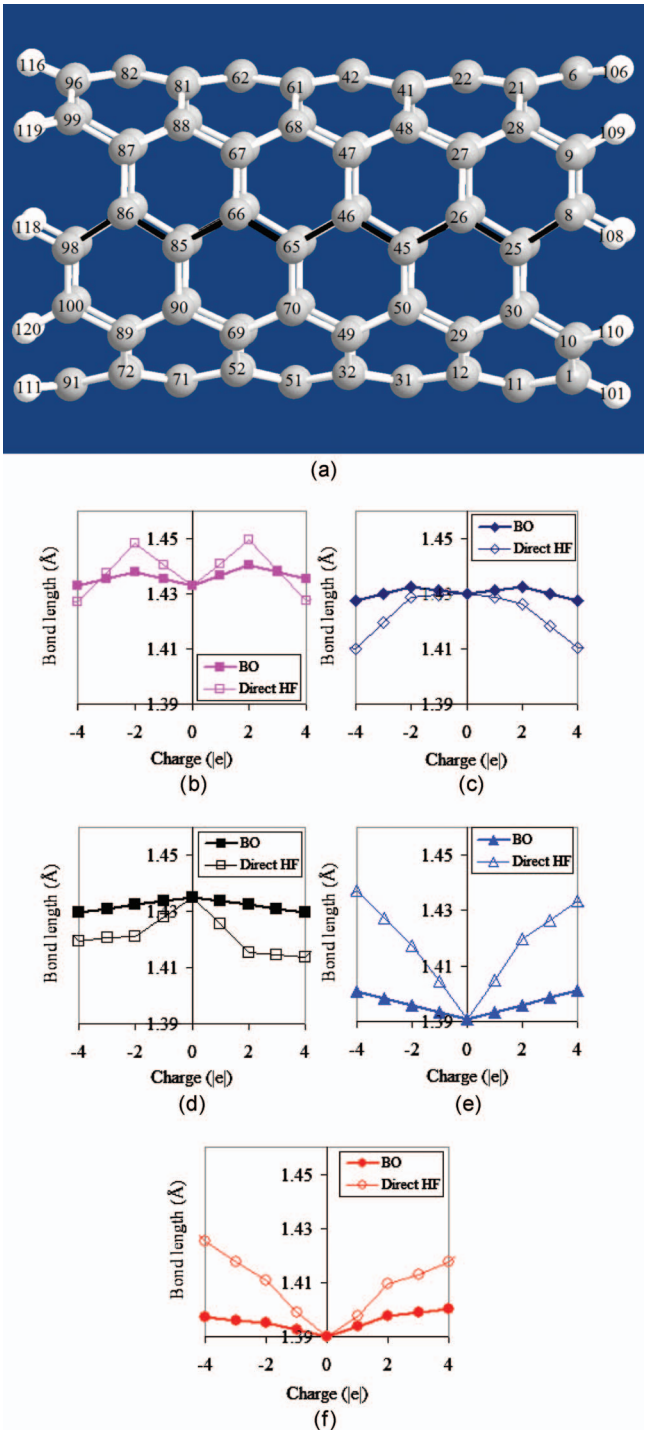

FIG. 4. (a) The structure of the CNT segment under study with atoms numbered and bonds, whose lengths are studied, blackened. The lengths of the black bonds as a function of total CNT segment charge level, based directly on HF simulations and based on BO method: (b) 86–98, (c) 45–46, (d) 26–45, (e) 46–65, and (f) 85–86.

ad hoc and finding a comparable parameter from our BO simulations would require some knowledge about all three coordinates of each atom in space, which would be hard to obtain using simple geometric arguments similar to those used to find axial strain. Nevertheless, it is informative to find an effective diameter for the CNT segment by adding up the circumferential contributions of various bonds near the middle of the CNT segment, and dividing it by π. Figure 5

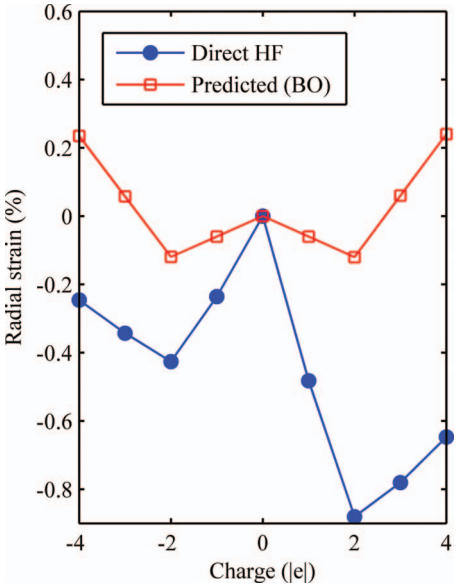

FIG. 5. Radial strain (%) calculated directly from HF simulations and calculated based on the BO approach.

compares the results for charge levels from −4 to +4 |e| with radial strain results from Fig. 1. It can be seen that the qualitative expansion-contraction behavior is once again predicted correctly.

The present case-study shows the potential for using our proposed method to predict the electromechanical actuation in various CNT-based structures or other large molecules. The hope is that using our theory, the actuation behavior of such structures (i.e., expansion/contraction in a given direction) can be predicted once the spatial distributions of their MOs are known. If the structure is changed, for example by using a longer or shorter CNT segment, the spatial distribution of its MOs may change. However, presumably the actuation behavior would also be different for the new structure. The evidence from the present case study suggests that we should still be able to use the spatial distribution of MOs and the concept of BO to at least qualitatively predict the actuation behavior of the new structure. Even in the limit of an infinitely long CNT the MOs will have a particular spatial distribution. Therefore, regardless of whether the spatial distributions of the HOMO and LUMO are distinct or identical, the present theory can still be applied to the spatial distribution of the MOs of the infinitely long CNT to at least qualitatively predict the effect of BO on actuation.

V. CONCLUSIONS AND FUTURE WORK

A method is proposed to predict the nonelectrostatic part of the electromechanical actuation response of a single (5,5) CNT segment based on the spatial distribution of MOs. Locally bonding and locally antibonding MOs were defined for the CNT segment structure based on analogy with bonding and antibonding orbitals in diatomic molecules. It was found that when an electron is added to a MO, the bonds that are locally bonding with respect to that orbital tend to contract, while the bonds that are locally antibonding with respect to the orbital tend to expand. The direction of the overall actuation, which had previously been found to be nonmonotonic, is explained based on the above proposition and the general alignment of the expanding and contracting bonds with respect to the axis or circumference of the CNT segment. This analysis is based on data for just one armchair nanotube. It would be important to show if the BO approach still works on zigzag and chiral nanotube. Such studies would be the subject of future publications.

ACKNOWLEDGMENTS

The authors thank the Natural Sciences and Engineering Research Council of Canada for support through the Discovery Grant program and a Postgraduate Scholarship granted to R.K.P. Special thanks to Dr. Fernando R. Clemente and Gaussian technical support staff for their timely help with Gaussian simulation issues, to Westgrid Canada for providing computational facilities, and to Professor George Sawatsky for a valuable discussion.

[1] T. T. Liu and X. Wang, Phys. Lett. A **365**, 144 (2007); X. B. Dai, H. Merlitz, and C. X. Wu, Eur. Phys. J. B - Condensed Matter and Complex Systems **54**, 109 (2006).
[2] R. H. Baughman, A. A. Zakhidov, and W. A. de Heer, Science **297**, 787 (2002).
[3] R. H. Baughman, C. X. Cui, A. A. Zakhidov, Z. Iqbal, J. N. Barisci, G. M. Spinks, G. G. Wallace, A. Mazzoldi, D. De Rossi, A. G. Rinzler, O. Jaschinski, S. Roth, and M. Kertesz, Science **284**, 1340 (1999).
[4] D. E. Nixon and G. S. Perry, J. Phys. C 1732 (1969).
[5] B. Vigolo, A. Penicaud, C. Coulon, C. Sauder, R. Pailler, C. Journet, P. Bernier, and P. Poulin, Science **290**, 1331 (2000).
[6] M. Zhang, K. R. Atkinson, and R. H. Baughman, Science **306**, 1358 (2004).
[7] T. Mirfakhrai, J. Oh, M. Kozlov, E. C.-W. Fok, M. Zhang, S. Fang, R. H. Baughman, and J. D. W. Madden, Smart Mater. Struct. **16**, S243 (2007); M. E. Kozlov, J. Oh, V. Seker, E. Kozlov, M. Zhang, S. Fang, R. Capps, E. Munoz, R. H. Baughman, T. Mirfakhrai, and J. D. W. Madden, *Electro-Mechanical Actuation of Carbon Nanotube Yarns, Sheets and Composites*, presented at the MRS fall meeting, 2005.
[8] M. J. Frisch, G. W. Trucks, H. B. Schlegel *et al.*, GAUSSIAN 03, Revision C.02 (Gaussian, Inc., Wallingford, CT, 2004).
[9] T. Mirfakhrai, R. Krishna-Prasad, A. Nojeh, and J. D. W. Madden, Nanotechnology **19**, 315706 (2008).
[10] C.-Y. Li and T.-W. Chou, Nanotechnology **17**, 4624 (2006).
[11] M. Orchin and H. H. Jaffe, *The Importance of Antibonding Orbitals* (Houghton, Cambridge, MA, 1967).
[12] R. C. Bochicchio, L. Lain, and A. Torre, Chem. Phys. Lett. **374**, 567 (2003).
[13] L. Pauling, J. Am. Chem. Soc. **69**, 542 (1947).
[14] C. A. Coulson and R. Taylor, Proc. Phys. Soc., London, Sect. A **65**, 815 (1952).
[15] T. Kakitani, Prog. Theor. Phys. **51**, 656 (1974).
[16] L. Pietronero and S. Strässler, Phys. Rev. Lett. **47**, 593 (1981).
[17] M. Verissimo-Alves, B. Koiller, H. Chacham, and R. B. Capaz, Phys. Rev. B **67**, 161401 (2003).